CHEMNANOMAT

Supporting Information

Antisite Defects and Chemical Expansion in Low-damping, High-magnetization Yttrium Iron Garnet Films

Jose Santiso, Carlos García, Cristian Romanque, Loïc Henry, Nicolas Bernier, Núria Bagués, José Manuel Caicedo, Manuel Valvidares, and Felip Sandiumenge*

S1: Analysis of the oxidation state of Fe ions

In the XAS measurement several spectral features are sensitive to the occupancy of Fe-3*d* levels. Since the $L_{2,3}$-edge systematically shifts to higher energy values for higher oxidation states, we first focus on the position of the main peaks [1]. As seen in Figure 1c, the L_3 spectrum shows a main peak located at an energy of 709.2 eV, preceded by a pre-peak at 708.0 eV, and the L_2 spectrum shows a broad double peak located at 722.7 eV. These values are in good agreement with those reported for Fe^{3+} ions: E(L_3): 709.5 eV (pre-peak at 708.0 eV) [2,3]. The measured energy difference E(L_2) – E(L_3) = 13.4 eV also agrees well with that reported for trivalent iron: 13.2 eV [3,4]. Corresponding values for Fe^{2+} ions are substantially smaller: E(L_3) = 707.8 eV and E(L_2) – E(L_3) = 12.8 eV [1,2]. The intensity ratio between the pre-peak and L_3 intensities, 0.40, is also consistent with the value found in the γ-Fe_2O_3 structure, and is known to rapidly rise with increasing the Fe^{2+} state [5,6]. Finally, a further signature of Fe^{2+} ions is the appearance of a pre-peak preceding the L_2 doublet [5,6], which is not observed. Thus, from this analysis we conclude that, within the first 2-5nm beneath the film surface sampled by the X-rays, Fe ions are in a trivalent state.

S2: Net lattice stretching caused by antisite defects

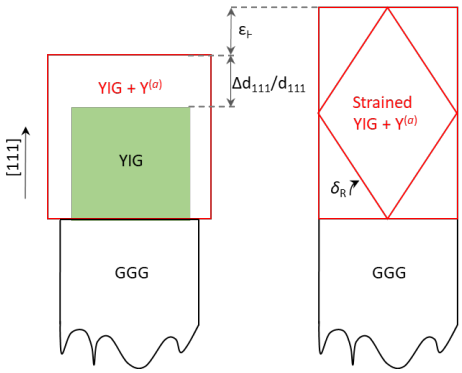

Figure S2: Schematics showing the effect of antisite defects on the misfit strain between the GGG substrate and the YIG film. For the (111) orientation, in-plane matching is materialized along the in-plane [01-1] and [2-1-1] crystallographic directions, leading to misfit values 5.7×10^{-4} and 5.9×10^{-4}, respectively. According to atomistic calculations, inserting one $Y^{(a)}$ excess defect per unit cell (8 f.u.) causes a 0.72% increase in volume [7], as indicated by the red square in the schematics (left panel). Thus, the misfit strain becomes compressive: -0.0018 and -0.0020 along [01-1] and [2-1-1], respectively. Forcing lattice matching at the interface (see right panel), causes a normal strain, $\varepsilon_\perp$, which can be obtained from the Poisson's ratio along the [111] direction,

$$\varepsilon_\perp = \frac{2\nu_{[111]}\varepsilon_\parallel}{\nu_{[111]} - 1}$$

Where

$$\nu_{[111]} = \frac{C_{11}^2 + C_{11}C_{12} - 2C_{12}^2 - 2C_{11}C_{44} + 8C_{12}C_{44}}{3(C_{11}^2 + C_{11}C_{12} - 2C_{12}^2 + 2C_{11}C_{44})}$$

Using elastic constants C_{11} = 268.0GPa, C_{12} = 110.6GPa and C_{44} = 76.6GPa [8], a biaxial Poisson's ration along the [111] direction of $\nu_{[111]}$ = 0.29 is obtained. Averaging the two misfit values: -0.0019, one obtains a tensile normal strain of $\varepsilon_{\perp}$ = 0.0015.

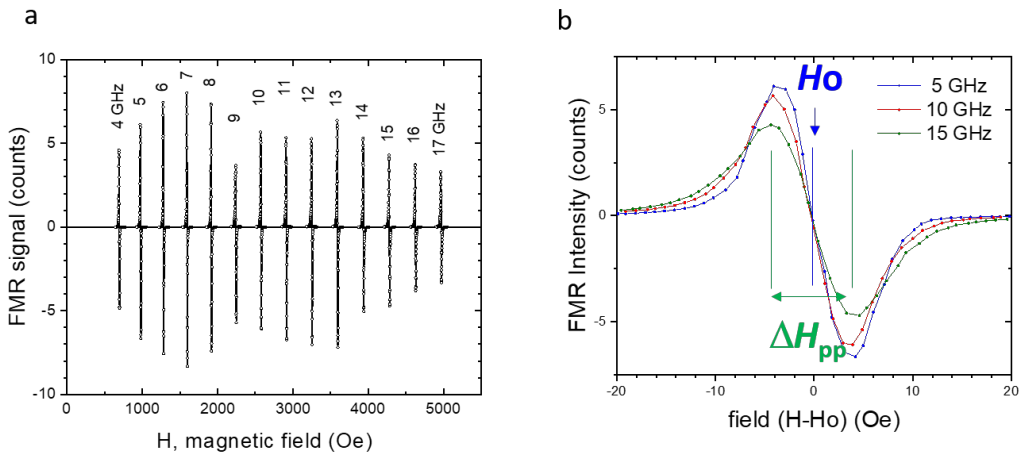

Figure S3: Ferromagnetic resonance was measured at room temperature by sweeping the applied magnetic field, *H*, at different excitation frequencies in the range from 4 to 17 GHz (with 1 GHz step). (a) depicts the variation of the resonance field with frequency for the whole frequency range. (b) shows in more detail the shape of the resonance curve for three different excitation frequencies: 5, 10 and 15 GHz, with the expected inverted double Lorentzian centered at the resonance field, H_0, and peak broadening (peak-to-peak width), ΔH_{pp}. The fact that the film shows only one resonance is an indication of the magnetic homogeneity of the sample. From the dependence of the resonance field with frequency it is possible to extract the gyromagnetic constant, γ, as well as the saturation magnetization of the sample, M_s, as depicted in Fig 5(a) in the main text. The magnitude of the resonance broadening is related to the spin wave propagation in the film and directly related to the Gilbert damping, α, as depicted in Fig.5(b) in the main text. Any deviation from a linear dependence should be related to the appearance of inelastic scattering of the spin waves caused by local magnetic inhomogeneities, often related to a two-magnon scattering process with magnitude Γ_0, which in this case is negligible, indicating the good quality of the sample.

References

[1] H. Tan, Jo Verbeeck, A. Abakumov, G. VanTendeloo, *Ultramicroscopy* **2012**, *116,* 24–33.

[2] L. A. J. Garvie and P. R. Buseck, Ratios of ferrous to ferric iron from nanometre-sized areas in minerals, *Nature* **1998**, *396*, 667-670.

[3] P. A. van Aken, B. Liebscher, and V. J. Styrsa, *Phys. Chem. Minerals* **1998**, *25*, 323-327.

[4] C. Colliex, T. Manoubi, C. Ortiz, *Phys. Rev. B* **1991**, *44*, 11402-114011.

[5] V. R. Galakhov, E. Z. Kurmaev, K. Kuepper, M. Neumann, J. A. McLeod, A. Moewes, I. A. Leonidov, V. L. Kozhevnikov, *J. Phys. Chem. C* **2010**, *114*, 5154–5159.

[6] H. B. Vasili, B. Casals, R. Cichelero, F. Macià, J. Geshev, P. Gargiani, M. Valvidares, J. Herrero-Martin, E. Pellegrin, J. Fontcuberta, G. Herranz, *Phys. Rev. B* **2017**, *96*, 014433.

[7] T. Su, S. Ning, E. Cho, and C. A. Ross, *Phys. Rev. Materials* **2021**, *5*, 094403.

[8] H Donnerberg and C R A Catlow, *J. Phys.: Condens. Matter* **1993**, *5* 2947.